

ORIGINAL RESEARCH

Tristetraprolin Prevents Gastric Metaplasia in Mice by Suppressing Pathogenic Inflammation



Jonathan T. Busada,^{1,4} Stuti Khadka,⁴ Kylie N. Peterson,¹ Sara R. Druffner,⁴ Deborah J. Stumpo,² Lecong Zhou,³ Robert H. Oakley,¹ John A. Cidlowski,¹ and Perry J. Blakeshear²

¹Molecular Endocrinology Group, ²Post-Transcriptional Gene Expression Group, ³Integrative Bioinformatics Support Group, National Institute of Environmental Health Sciences, National Institutes of Health, Research Triangle Park, North Carolina;

⁴Department of Microbiology, Immunology and Cell Biology, West Virginia University School of Medicine, Morgantown, West Virginia

SUMMARY

Aberrant gastric inflammation damages the stomach and induces gastric metaplasia (spasmolytic polypeptide-expressing metaplasia). Increased expression of the RNA binding protein tristetraprolin suppresses adrenalectomy-induced gastric inflammation and spasmolytic polypeptide-expressing metaplasia development.

GSE164349. (*Cell Mol Gastroenterol Hepatol* 2021;12:1831–1845; <https://doi.org/10.1016/j.jcmgh.2021.07.015>)

Keywords: gastric inflammation, adrenalectomy, SPEM, gastric cancer.

BACKGROUND & AIMS: Aberrant immune activation is associated with numerous inflammatory and autoimmune diseases and contributes to cancer development and progression. Within the stomach, inflammation drives a well-established sequence from gastritis to metaplasia, eventually resulting in adenocarcinoma. Unfortunately, the processes that regulate gastric inflammation and prevent carcinogenesis remain unknown. Tristetraprolin (TTP) is an RNA-binding protein that promotes the turnover of numerous proinflammatory and oncogenic messenger RNAs. Here, we assess the role of TTP in regulating gastric inflammation and spasmolytic polypeptide-expressing metaplasia (SPEM) development.

METHODS: We used a TTP-overexpressing model, the TTP Δ adenylate-uridylylate rich element mouse, to examine whether TTP can protect the stomach from adrenalectomy (ADX)-induced gastric inflammation and SPEM.

RESULTS: We found that TTP Δ adenylate-uridylylate rich element mice were completely protected from ADX-induced gastric inflammation and SPEM. RNA sequencing 5 days after ADX showed that TTP overexpression suppressed the expression of genes associated with the innate immune response. Importantly, TTP overexpression did not protect from high-dose-tamoxifen-induced SPEM development, suggesting that protection in the ADX model is achieved primarily by suppressing inflammation. Finally, we show that protection from gastric inflammation was only partially due to the suppression of *Tnf*, a well-known TTP target.

CONCLUSIONS: Our results show that TTP exerts broad anti-inflammatory effects in the stomach and suggest that therapies that increase TTP expression may be effective treatments of proneoplastic gastric inflammation. Transcript profiling;

Gastric adenocarcinoma is the third leading cause of cancer deaths worldwide.¹ Chronic inflammation is strongly correlated with gastric cancer development and typically is initiated by *Helicobacter pylori* infection or autoimmune gastritis.^{2,3} Chronic inflammation causes atrophic gastritis and loss of the acid-secreting parietal cells (oxyntic atrophy), leading to the development of spasmolytic polypeptide-expressing metaplasia (SPEM).⁴ These lesions are postulated to be the precursors of gastric adenocarcinoma.^{5–7} A host of immune pathways and cytokines have been associated with SPEM development and gastric carcinogenesis.⁸ Excessive expression of proinflammatory cytokines such as interferon gamma, tumor necrosis factor alpha (TNF), and interleukin (IL)1B induce SPEM and dysplasia.^{4,9–12} In contrast, disruption of cytokines that exert anti-inflammatory effects, such as IL10 or IL27, may increase cancer risk.^{13–15} Recent studies by our group have uncovered the broad anti-inflammatory role of the steroid hormones glucocorticoids and androgens within the stomach.^{16,17} Loss of these hormones leads to spontaneous activation of the innate immune response, driving SPEM development. However, the mechanisms that regulate gastric inflammation remain poorly defined.

Abbreviations used in this paper: ADX, adrenalectomy; ARE, adenylate-uridylylate rich element; CTNNB1, β -catenin; DEG, differentially expressed gene; FPKM, fragments per kilobase of transcript per million mapped reads; GO, gene ontology; GSEA, gene set enrichment analysis; GSII, *Griffonia simplicifolia*; HDT, high-dose tamoxifen; IL, interleukin; IPA, Ingenuity Pathway Analysis; KO, knockout; MIST1, basic helix-loop-helix family, member a15; mRNA, messenger RNA; RNAseq, RNA sequencing; SPEM, spasmolytic polypeptide-expressing metaplasia; TNF, tumor necrosis factor; TTP, tristetraprolin; UTR, untranslated region; WT, wild-type.

Most current article

© 2020 The Authors. Published by Elsevier Inc. on behalf of the AGA Institute. This is an open access article under the CC BY license (<http://creativecommons.org/licenses/by/4.0/>).

2352-345X

<https://doi.org/10.1016/j.jcmgh.2021.07.015>

Tristetraprolin (TTP) is a member of a small family of RNA binding proteins and is encoded by the gene *Zfp36*.^{18,19} Proteins of the TTP family are characterized by highly conserved tandem zinc finger domains that bind to AU rich-elements (AREs) in the 3' untranslated region (UTR) of target messenger RNAs (mRNAs).^{20,21} TTP binding initiates deadenylation and degradation of the target transcript.²¹ The ideal binding sequence, UUAUUUAUU or its variants, recognized by TTP, is found in a host of transcripts that encode proinflammatory cytokines, chemokines, and oncogenes.^{22,23} Loss of TTP expression increases the half-life of target mRNAs, and TTP expression is reduced or lost in numerous cancers, including gastric cancer.^{23,24} Germline *Zfp36* knockout (KO) mice show numerous systemic inflammatory pathologies such as dermatitis, arthritis, autoimmunity, and myeloid hyperplasia, all of which are linked to aberrant expression of the proinflammatory cytokine TNF.²⁵

TTP expression is rapidly induced during inflammation, in which it regulates the intensity and duration of the inflammatory response.²⁶ However, TTP expression usually is transient, in part owing to binding sites within the TTP transcript that allow the TTP protein to negatively regulate its own expression.²⁷ Mice with a germ-line deletion of a 136-base ARE within the TTP mRNA 3' UTR (TTP Δ ARE) have enhanced TTP mRNA stability and moderately increased TTP protein expression in their tissues but are phenotypically normal during normal vivarium conditions.²⁸ However, TTP Δ ARE mice are resistant to experimental models of imiquimod-induced dermatitis, collagen antibody-induced arthritis, experimental autoimmune encephalomyelitis, bacterial gingivitis and dental bone erosion, inflammatory lung damage, experimental autoimmune uveitis, and chemically induced skin carcinogenesis.^{29–32}

We previously showed that glucocorticoids are master regulators of gastric inflammation. Systemic removal of endogenous glucocorticoids by ADX triggers massive, spontaneous gastric inflammation and SPEM.¹⁷ Adrenalectomy is a useful model to study factors that participate in gastric inflammation and SPEM development. In this study, we used the ADX model to investigate the effects of enhanced TTP expression on gastric inflammation and metaplasia. We found that increased, regulated, whole-body TTP expression completely blocked the development of gastric inflammation and metaplasia after bilateral ADX. Surprisingly, protection from ADX-induced gastric inflammation was not recapitulated in *Tnf* KO mice, suggesting that TTP regulation of gastric inflammation is more complex than suppressing a single proinflammatory cytokine. Our results suggest that treatments that increase TTP protein expression may effectively treat gastric inflammation and potentially protect against neoplasia development.

Results

TTP Suppresses Adrenalectomy-Induced Gastric Inflammation

Gastric inflammation is associated with the development of gastritis, oxyntic atrophy, and metaplasia. TTP enhances the turnover of numerous proinflammatory mRNAs such as

those encoding TNF.^{22,25} We hypothesized that enhanced systemic TTP expression could protect mice from gastric inflammation and metaplasia. To test this hypothesis, we used TTP Δ ARE mice in which a 136-base AU-rich instability region was deleted from the 3' UTR of the gene encoding TTP, *Zfp36*.²⁸ As previously reported in other tissues,²⁸ we confirmed that germline deletion of the ARE region results in the accumulation of TTP mRNA in the mouse gastric fundus at 2 months of age (Figure 1A). We previously showed that adrenalectomy (ADX) rapidly induces spontaneous gastric inflammation and SPEM.¹⁷ We used bilateral ADX to assess gastric inflammation and SPEM development in TTP Δ ARE mice (Figure 1B). As expected, wild-type (WT) control mice showed prominent inflammation within the gastric corpus 2 months after ADX (Figure 1C). In contrast, both TTP Δ ARE heterozygous and homozygous mice were protected from increased inflammation. We previously have shown that ADX-induced gastric inflammation is composed predominately of macrophages and eosinophils.^{16,17} Analysis of the WT mice showed 4.7-fold and 28-fold increases in gastric macrophages and eosinophils 2 months after ADX, respectively (Figure 1D). In contrast, neither TTP heterozygous mice nor homozygous mice showed a significant increase in inflammatory cells. These data indicate that increased systemic TTP expression from normally regulated *Zfp36* can protect the stomach from ADX-induced chronic inflammation.

TTP Protects Mice From SPEM Development

SPEM develops in response to glandular damage such as oxyntic atrophy and is a putative precursor of gastric adenocarcinoma.³³ Inflammation potently induces SPEM development.¹⁷ Because TTP Δ ARE mice were resistant to ADX-induced inflammation, we asked whether increased TTP expression could prevent the development of oxyntic atrophy and metaplasia. The gross morphology of sham-operated TTP Δ ARE heterozygous and homozygous mice was indistinguishable from sham-operated WT mice (Figure 2A), and there were no significant differences in the number of parietal cells or chief cells (Figure 2B). Two months after ADX, WT mice had lost 82% of their parietal cell population and 99% of their mature chief cells (Figure 2). Moreover, WT mice showed prominent mucous cell hyperplasia within the gastric corpus, identified by an increase in *Griffonia simplicifolia* (GSII) lectin staining, which binds to mucin 6. In contrast to ADX-WT mice, neither TTP Δ ARE heterozygous nor homozygous mice showed a significant change in their parietal and chief cell populations, and both genotypes had normal gastric morphology 2 months after ADX (Figure 2).

Oxyntic atrophy, loss of the mature chief cell marker BHLHA15 (also known as MIST1), and expansion of GSII+ cells are among the defining characteristics of SPEM. We confirmed SPEM development by immunostaining for the de novo SPEM marker CD44v9, a splice variant of CD44.³⁴ Although there was widespread staining of CD44v9 in ADX WT mice, CD44v9 was not detected within the gastric glands of ADX TTP Δ ARE mice (Figure 3A). Re-entry into the

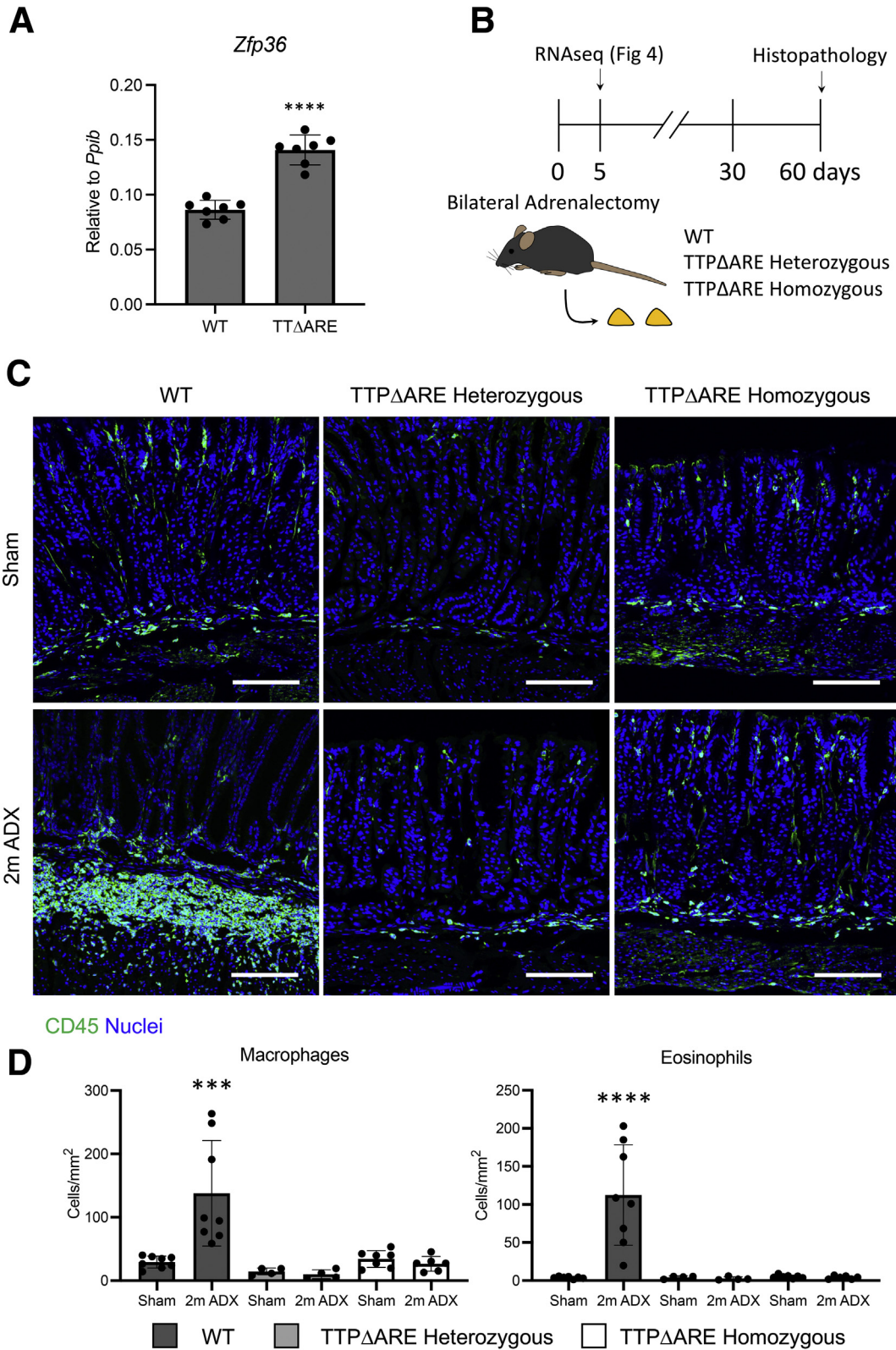


Figure 1. Increased levels of TTP prevent ADX-induced gastric inflammation. (A) qRT-PCR for TTP mRNA within the gastric corpus. (B) Experimental model. (C) Representative immunostaining of the gastric corpus from WT, TTP Δ ARE heterozygous, and TTP Δ ARE homozygous mice 2 months after sham surgery or ADX. Gastric sections were stained with CD45 antibodies (green) and nuclei were stained with 4',6-diamidino-2-phenylindole. Scale bars: 100 μ m. $n \geq 7$ mice/group. (D) Quantitation of macrophages (CD68 and CD45 double-positive) and eosinophils (Siglec F and CD45 double-positive). $n \geq 4$ mice/group. (A and D) Data are means \pm SD. P values were determined by (A) an unpaired Student t test or (D) 1-way analysis of variance with a post hoc Tukey t test. *** $P \leq .001$ and **** $P \leq .0001$.

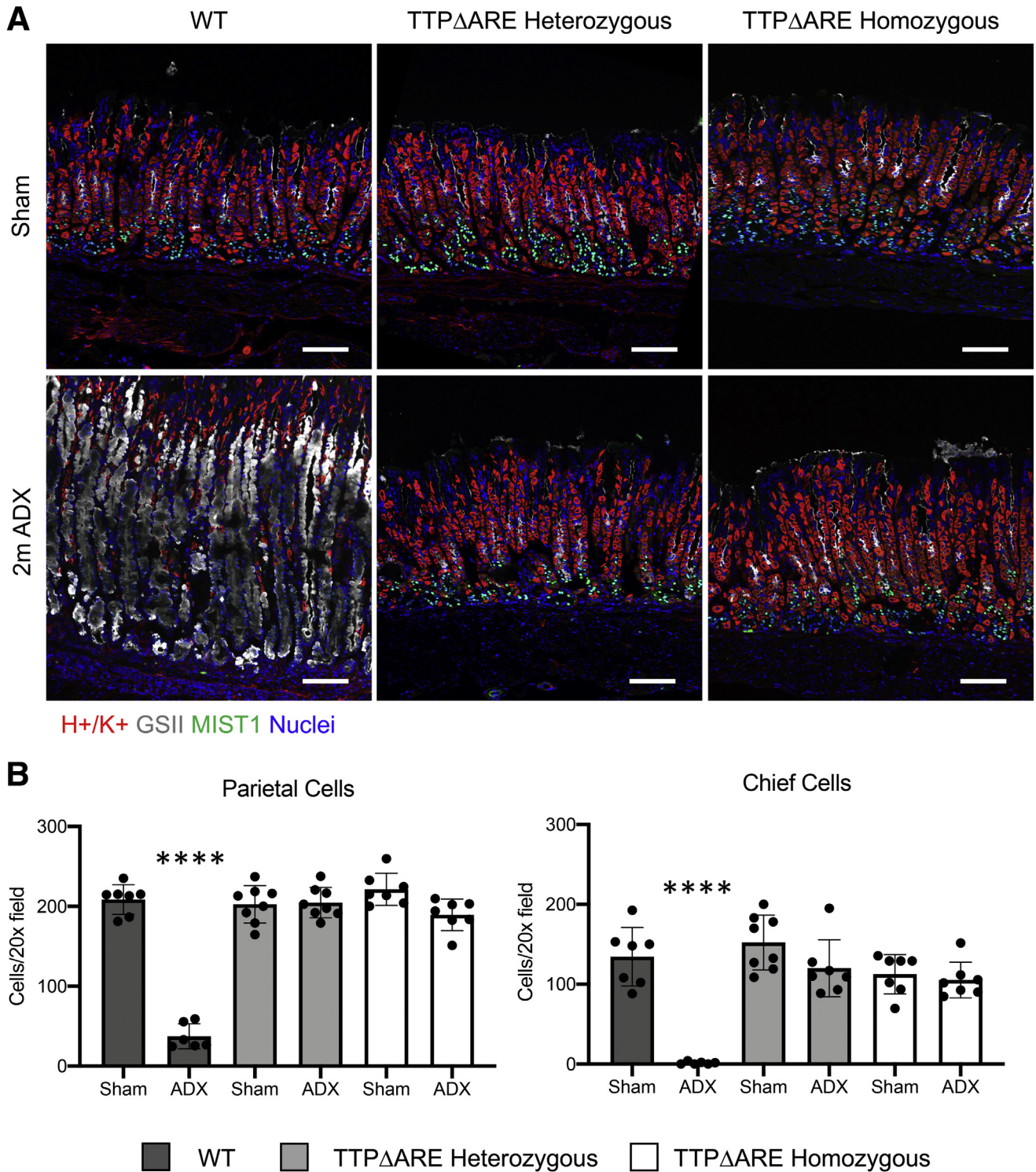


Figure 2. Increased levels of TTP protect the stomach from ADX-induced pathogenic inflammation. (A) Representative immunostaining of the gastric corpus from WT, TTP Δ ARE heterozygous, and TTP Δ ARE homozygous mice killed 2 months after sham surgery or ADX. Gastric sections were probed for ATP4B (parietal cells, red), MIST1 (chief cells, green), and GSII lectin (mucous neck cells, grey). Nuclei were stained with 4',6-diamidino-2-phenylindole. Scale bars: 100 μ m. (B) Quantitation of the number of parietal cells and chief cells observed per 20 \times field ($n \geq 6$ mice/group). Data are means \pm SD, P values were determined by 1-way analysis of variance with a post hoc Tukey t test. **** $P \leq .0001$.

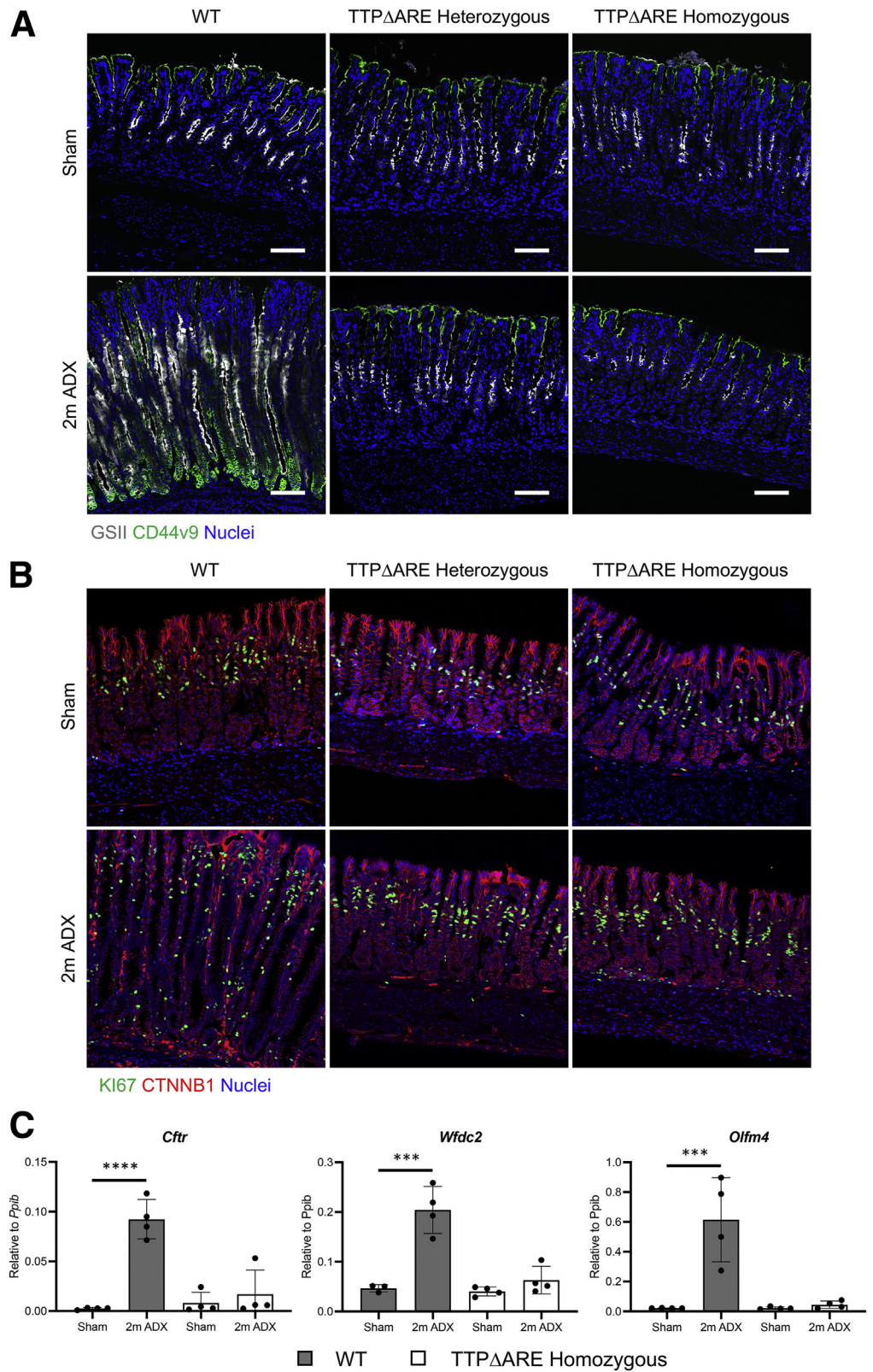


Figure 3. Increased levels of TTP prevent SPEM development. (A and B) Representative immunostaining of the gastric corpus from WT, TTP Δ ARE heterozygous, and TTP Δ ARE homozygous mice 2 months after sham surgery or adrenalectomy. Gastric sections were probed for (A) the SPEM marker CD44v9 (green) and the lectin GSII (mucous neck cells, grey) or (B) with Ki67 (green) and CTNNB1 (red, epithelial cells). Nuclei were stained with 4',6-diamidino-2-phenylindole. Scale bars: 100 μ m. $n \geq 6$ mice/group. (C) qRT-PCR of the indicated SPEM marker genes using RNA isolated from the gastric corpus ($n \geq 4$ mice/group). Data are means \pm SD. P values were determined by 1-way analysis of variance with a post hoc Tukey t test. *** $P \leq .001$ and **** $P \leq .001$.

cell cycle accompanies chief cell transdifferentiation.^{35,36} We performed co-immunofluorescence for Ki67 and β -catenin (CTNNB1) to identify proliferative epithelial cells. In sham mice, proliferation was restricted to the gland isthmus, which is widely regarded as the stem cell compartment within the gastric corpus (Figure 3B). In contrast, 2 months after ADX, WT mice showed numerous Ki67+ cells throughout the neck and base. However, proliferation remained unchanged 2 months after ADX in TTP Δ ARE heterozygous and homozygous mice. In addition, we performed quantitative reverse-transcription polymerase chain reaction (qRT-PCR) on a panel of transcripts from the advanced SPEM-associated genes *Cftr*, *Wfdc2*, and *Olfm4*.^{37,38} Consistent with the increase in CD44v9 staining, there was significant induction of all 3 SPEM markers in ADX WT mice (Figure 3C). However, these transcripts did not significantly increase in TTP Δ ARE homozygous mice. These results show that increased TTP expression protected the mice from oxyntic atrophy and SPEM development.

TTP Suppresses the Induction of Proinflammatory Gene mRNAs After ADX

Because TTP Δ ARE mice were protected from ADX-induced gastric inflammation and SPEM, we next used RNA sequencing (RNAseq) to examine their gastric transcriptomes 5 days after ADX (Figure 1B). We used this early time after ADX to avoid secondary changes caused by the anatomic alterations seen in long-term ADX mice. Moreover, there was limited gastric inflammation 5 days after ADX, as shown by a modest increase in the pan-immune cell marker *Ptprc* (CD45) and the pan macrophage marker *Cd68* (Figure 4A). RNAseq showed significant increases in inflammatory gene expression 5 days after ADX in WT mice. Gene set enrichment analysis (GSEA) comparing sham WT vs ADX WT groups showed significant enrichment of mRNAs associated with the Gene Ontology (GO) inflammatory response pathway (Figure 4B). Surprisingly, there also was significant enrichment of inflammatory genes 5 days after ADX in TTP Δ ARE homozygous mice. However, the normalized enrichment score was 6.36 in the WT group compared with 5.02 in the TTP Δ ARE group, suggesting moderately increased inflammation within the WT group. Moreover, a comparison of the ADX WT group with the ADX TTP Δ ARE group showed greater activation of inflammatory response pathways in ADX WT mice (Figure 4B). Next, we ranked the GSEA data and found that the GO innate immune response pathway was the seventh highest activated pathway in the WT group (normalized enrichment score, 5.32) (Figure 4C). In contrast, this pathway was ranked 46th in the TTP Δ ARE group (normalized enrichment score, 3.97). Comparison of the WT ADX group with the TTP Δ ARE ADX group showed significant positive enrichment (Figure 4C), suggesting increased innate immune system activation in WT ADX mice.

Macrophages have been shown previously to be required to induce SPEM development.^{17,39} Therefore, we next analyzed the differentially expressed gene (DEG) lists using Ingenuity Pathway Analysis (IPA) to assess transcripts

associated with macrophage activation. IPA predicted significant activation of the "Activation of Macrophages" pathway in ADX WT mice (activation z-score, 2.43) (Figure 4D). However, this pathway was not significantly activated in ADX TTP Δ ARE mice. Importantly, GSEA showed that pathways associated with adaptive immunity, such as the GO adaptive immune response (Figure 4E) and gene GO lymphocyte activation (Figure 4F), were activated equivalently in both WT and TTP Δ ARE mice. These results are consistent with published reports that mature lymphocytes are dispensable for inducing SPEM development.¹⁷

Transcripts Containing AREs Are Only a Small Portion of the ADX-Induced Genes

TTP is an RNA binding protein that binds to adenylate-uridylylate-rich target sequences in mRNAs before promoting the turnover of those mRNAs. RNAseq showed 760 DEGs between the sham WT and ADX WT groups. In contrast, there were only 490 DEGs between the sham TTP Δ ARE mice and ADX TTP Δ ARE groups (Figure 5A). Of the DEGs, 189 genes were regulated in both groups. We screened the transcripts that were up-regulated by ADX in the WT group for the presence of ideal TTP binding sequences (UUAUUUAU and UAUUUUAU). We identified 94 mRNAs that contained a potential TTP binding motif (Figure 5B). Up-regulation of 93 of these transcripts was blunted significantly in ADX TTP Δ ARE mice, indicating that TTP may enhance the degradation of these transcripts. Importantly, there were established TTP targets among the 94 ARE-containing transcripts, such as the mRNA encoding *Tnf*, and inflammatory genes associated with SPEM development, including *Il13*. *Il13* is potently induced by the alarmin IL33.⁴⁰ Interestingly, we found that *Il13* expression was increased significantly only in TTP Δ ARE mice 5 days after ADX (Figure 5C). Consistent with this increase, we did not identify an ARE within the *Il13* transcript, suggesting it may not be a direct TTP target. In contrast, *Il13*, which does contain potential TTP binding sites, was blunted significantly in ADX TTP Δ ARE mice; thus, TTP suppression of *Il13* may disrupt macrophage activation. Together, these data show that TTP directly regulates numerous proinflammatory genes within the stomach.

Tnf Knockout Mice Are Partially Protected From ADX-Induced SPEM

TNF- α is a prominent proinflammatory cytokine produced by macrophages and other leukocytes. Aberrant TNF production is associated with inflammatory disease within the gastrointestinal tract, and may increase the risk of gastric cancer.^{11,41} Moreover, *Tnf* mRNA is an established TTP target, and germline *Zfp36* KO mice have systemic inflammation attributed in part to excessive TNF.^{20,25} We hypothesized that suppression of *Tnf* in TTP Δ ARE mice may protect against ADX-induced inflammation and metaplasia. Therefore, we adrenalectomized *Tnf* KO mice and assessed their stomachs 2 months after surgery. Interestingly, *Tnf* KO mice showed only intermediate protection from SPEM (Figure 6A and B). In ADX *Tnf* KO mice, there were regions

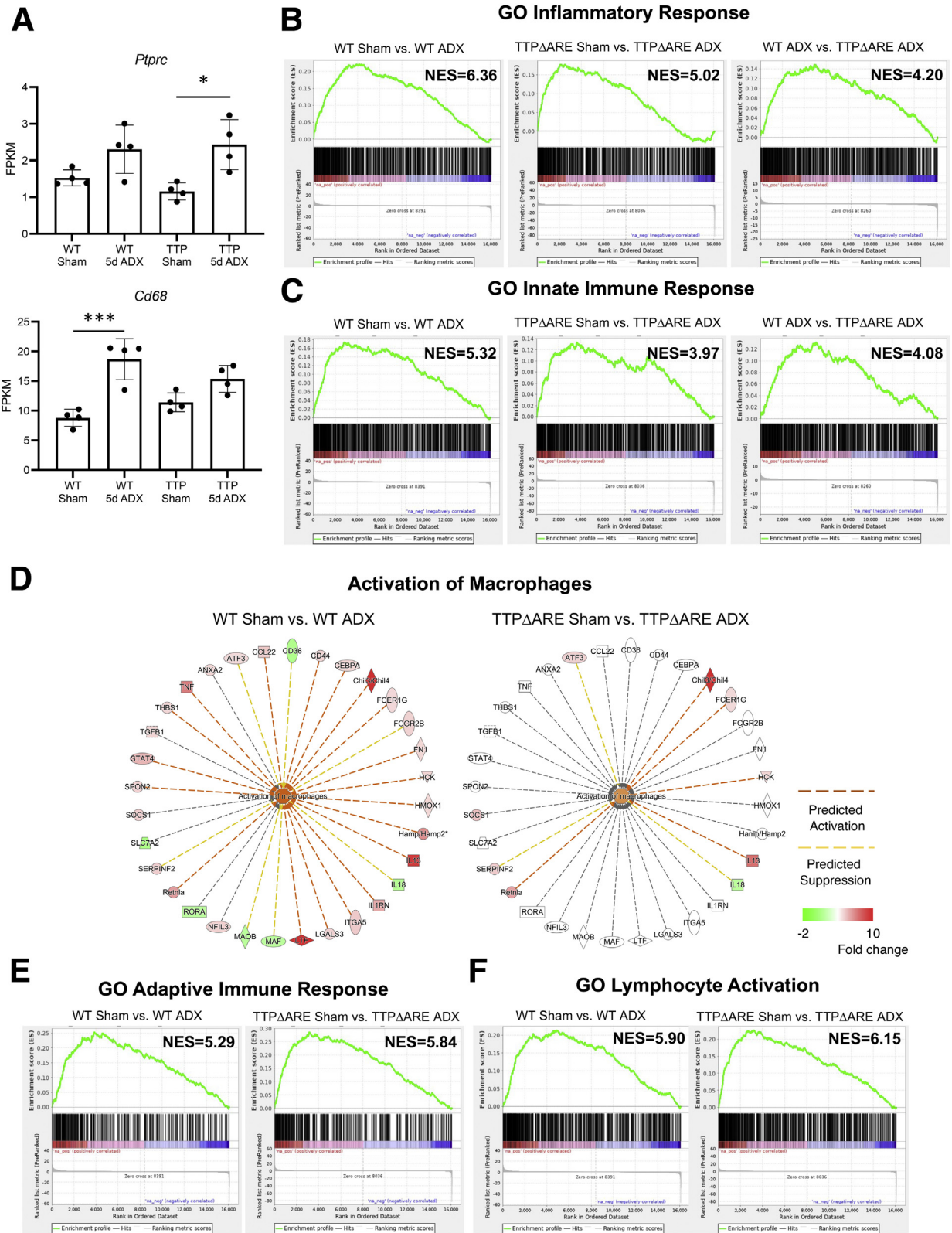


Figure 4. Increased TTP expression elicits broad suppression of inflammatory genes within the stomach of adrenalectomized mice. Shown are RNAseq data from total cellular RNA isolated from the gastric corpus of WT and TTP Δ ARE homozygous mice killed 5 days after sham surgery or ADX. (A) FPKM values for the indicated genes. *P* values were determined by 1-way analysis of variance with a post hoc Tukey *t* test. **P* \leq .05 and ****P* \leq .001. (B, C, E, and F) GSEA of the significantly regulated genes comparing adrenalectomized WT mice with adrenalectomized TTP mice. (D) IPA of the total number of significantly regulated genes in sham vs adrenalectomized WT mice and TTP mice, respectively. *n* = 4 mice/group. NES, normalized enrichment score.

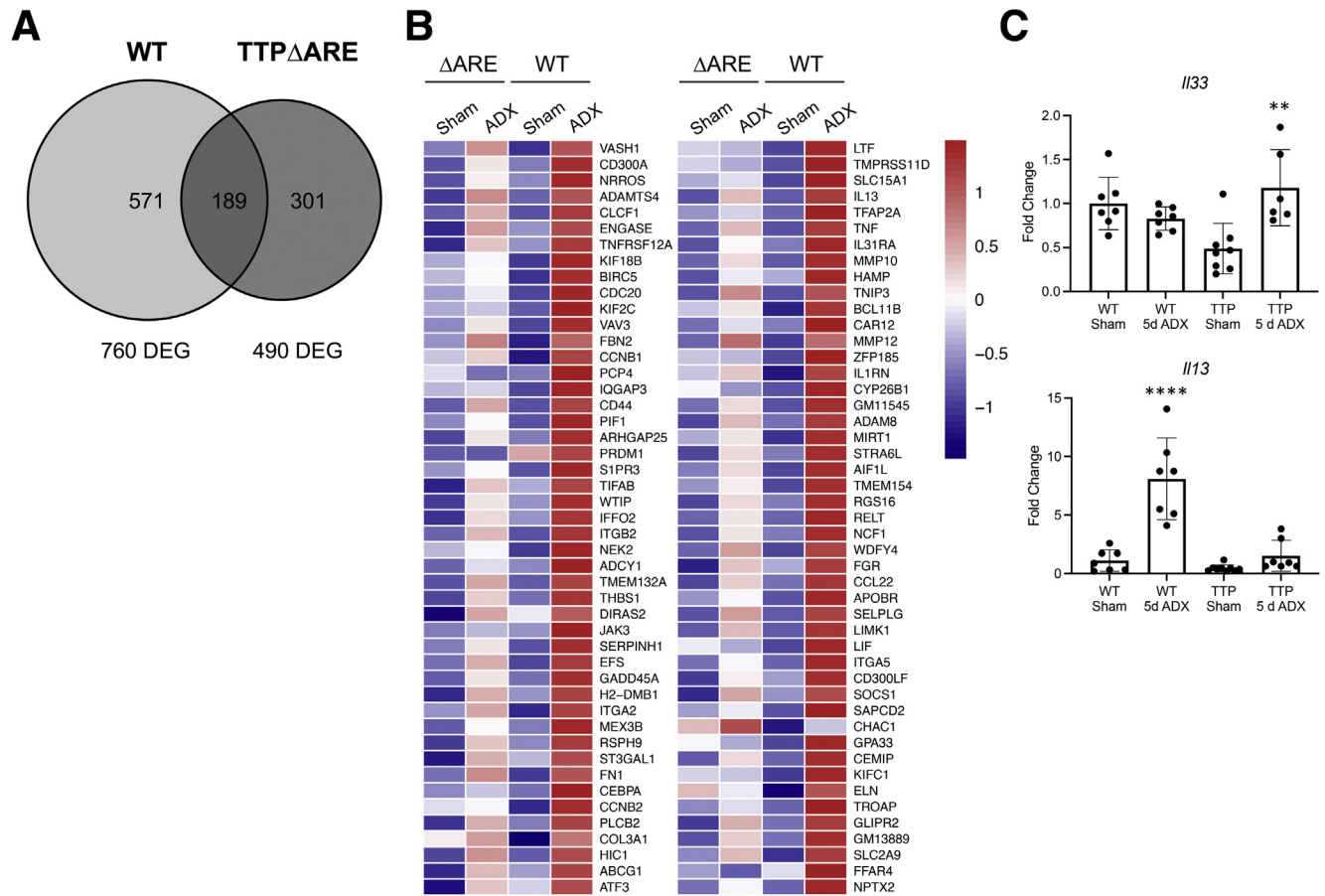


Figure 5. ARE-containing mRNAs are a small proportion of the DEGs in the stomach. (A) Venn diagram of the total number of DEGs in the gastric corpus 5 days after ADX. (B) Heatmap visualizing ARE-containing mRNAs in the indicated data sets. Transcripts were up-regulated significantly in ADX WT mice compared with sham WT mice. Scale is z-score minimum/maximum within the data set. (C) qRT-PCR of RNA isolated from the gastric corpus 5 days after sham or ADX surgery. $n \geq 6$ mice/group. Data are means \pm SD. P values were determined by 1-way analysis of variance with a post hoc Tukey t test. $**P \leq .01$ and $****P \leq .0001$.

of the gastric corpus that appeared identical to sham controls, with the normal complement of parietal and chief cells, and that were negative for the SPEM marker CD44v9 (Figure 6A). In contrast, other regions of the lesser curvature appeared identical to sections from the ADX WT mice (Figure 6A, far right panel). We quantitated the number of parietal and chief cells present in both normal and SPEM regions. Quantitation showed that although ADX *Tnf* KO mice showed a significant loss of parietal and chief cells relative to sham controls, these effects were diminished significantly compared with ADX WT mice (Figure 6B). In addition to stomach inflammation, ADX WT mice developed splenomegaly (Figure 6C and D), a classic feature of ADX in rodents.⁴² However, TTP Δ ARE homozygous spleen weights did not differ significantly from WT mice 2 months after ADX. Surprisingly, *Tnf* KO completely rescued the splenomegaly observed in ADX WT mice. Together, these data indicate that although *Tnf* contributes to SPEM development, there likely are redundant mechanisms that control pathogenic gastric inflammation. Moreover, these results show that TTP's protective effects in the stomach are the

result of broad anti-inflammatory effects beyond the suppression of *Tnf*.

TTP Does Not Prevent High-Dose-Tamoxifen-Induced SPEM Development

SPEM development occurs in response to glandular damage within the gastric corpus. Adrenalectomy induces SPEM development by triggering massive gastric inflammation.^{16,17} Our results show that TTP overexpression suppresses ADX-induced gastric inflammation. We hypothesized that TTP protected from SPEM by regulating gastric inflammation. To test this hypothesis, we used the high-dose tamoxifen (HDT) model. HDT induces chief cell transdifferentiation toward the SPEM lineage by killing parietal cells and is largely noninflammatory.^{43,44} WT and TTP Δ ARE homozygous mice were treated with HDT 3 times over 72 hours, and stomachs were collected 24 hours after the final dose. There were no morphologic differences between the stomachs of vehicle-treated WT and TTP Δ ARE mice (Figure 7A). As expected, HDT treatment induced nearly

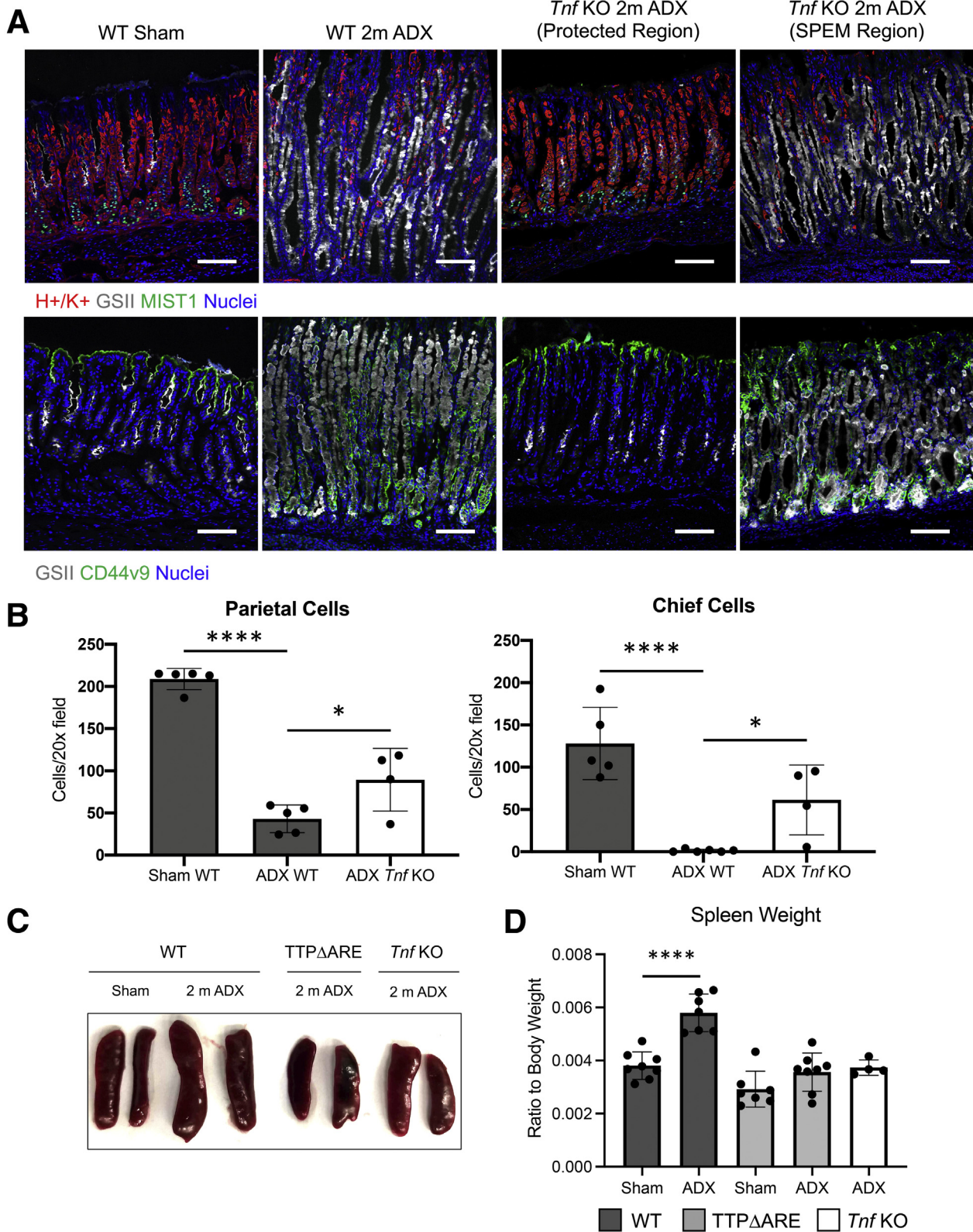


Figure 6. *Tnf* KO mice are partially protected from ADX-induced gastric inflammation (A) Representative images of stomachs taken from WT and *Tnf* KO mice killed 2 months after sham surgery or ADX. Scale bars: 100 μ m. (B) Quantitation of the number of parietal cells and chief cells observed per 20 \times field ($n \geq 4$ mice/group). (C) Representative images of spleens from mice killed 2 months after sham surgery or ADX. (D) Ratio of spleen weight normalized to total body weight. Data are means \pm SD. *P* values were determined by 1-way analysis of variance with a post hoc Tukey *t* test. **P* \leq .05 and *****P* \leq .0001.

complete oxyntic atrophy in both genotypes. Importantly, loss of mature chief cells, denoted by loss of MIST1 staining (Figure 7A) and *Gif* mRNAs (Figure 7B) was equivalent in both HDT-treated WT and TTP Δ ARE mice. Moreover, there was concurrent induction of the SPEM markers CD44v9 as well as *Cftr* mRNAs. These results show that TTP overexpression does not directly inhibit SPEM development and suggests that SPEM protection occurs through inhibition of the intensity and type of inflammation.

Discussion

Post-transcriptional regulation of gene expression by RNA binding proteins is critical for maintaining cellular and tissue homeostasis. Dysregulation of RNA binding proteins is associated with a host of diseases including cancer.⁴⁵ *Zfp36* encodes a zinc finger RNA binding protein, TTP, that binds to ARE-containing mRNAs and destabilizes them by recruiting deadenylases, thus promoting mRNA decay.⁴⁶ It has been estimated that approximately 26% of human mRNA 3' UTRs contain at least a single minimal TTP family binding site, UAUUUU or UAUUUUU, and disruption of TTP family members has been associated with inflammatory disorders and cancer.^{23,48-50} TTP is a critical regulator of numerous proinflammatory cytokines. TTP KO mice develop multisystem inflammatory disease that is largely caused by excessive TNF expression.^{23,25,51} In contrast, increased TTP expression confers resistance to numerous inflammatory pathologies including arthritis and dermatitis.²⁸⁻³⁰ Here, we report that knockin mice that have regulated increases in TTP levels throughout the body are protected from ADX-induced gastric inflammation and SPEM. Our results suggest that TTP could be a master regulator of gastric inflammation, and therapies that lead to increased TTP protein levels may be effective at treating gastric inflammation.

Chronic inflammation is strongly associated with gastric cancer development. Within the stomach, inflammation induces a well-defined histopathologic progression in which stomach damage leads to gastric atrophy, metaplasia, dysplasia, and adenocarcinoma.⁶ SPEM is a potentially preneoplastic form of metaplasia that develops in response to damage within the gastric corpus that also may serve as a healing mechanism.^{5,33} However, in the setting of prolonged damage, such as during chronic inflammation, SPEM becomes increasingly proliferative and eventually may progress toward carcinogenesis.⁸ We found that TTP overexpression protected mice from gastric inflammation and SPEM development. We used ADX as a model to challenge the TTP Δ ARE mice. In WT mice, ADX triggered massive spontaneous inflammation of the gastric corpus followed by SPEM development. Both homozygous and heterozygous TTP Δ ARE mice were completely protected from ADX-induced gross inflammation and SPEM development. We previously reported that suppressing gastric inflammation by depleting macrophages in ADX WT mice protects them from SPEM development.¹⁷ Thus, it is likely that TTP prevents SPEM development by suppressing inflammation. Importantly, we found that TTP

overexpression did not affect HDT-induced SPEM development. These results suggest that TTP does not directly inhibit SPEM development and that protection from SPEM in the ADX model likely occurs by inhibiting inflammation. Our results suggest that therapies that elicit even a modest increase in TTP expression may effectively control gastric inflammation.

TTP primarily functions by binding to specific AREs within the 3' UTR of target mRNAs, eventually promoting the degradation of the mRNA.⁵² Our RNAseq studies showed that TTP potently suppressed genes associated with macrophage activation in ADX mice. Importantly, TTP regulates the expression of IL13 and TNF α , cytokines that have been implicated in inducing SPEM development.^{24,40} Our RNAseq data showed that 33% of DEG transcripts in ADX WT mice contained potential TTP binding sites, including *Tnf* and *Il13*. TTP regulation of *Il13* may be an important mechanism protecting from SPEM. Within the stomach, *Il13* is potently expressed by type 2 innate lymphoid cells.¹⁶ In response to gastric epithelial damage, *Il13* is induced by IL33, which is released from the surface epithelial cells. IL13 drives alternative macrophage activation, which in turn drives SPEM development.^{40,53} Several recent studies have reported that IL33 is a critical mediator of SPEM development, and *Il13* KO mice are resistant to experimental SPEM models.^{16,40,53,54} Interestingly, *Il13* induction was greater in ADX TTP Δ ARE mice than in WT mice, and our analysis did not identify any TTP binding sites within the *Il13* gene, suggesting that TTP may not directly regulate *Il13* expression. Thus, TTP suppression of *Il13* may be important for disrupting macrophage activation and protecting from SPEM development. However, given that TTP can regulate other cellular pathways, including those involving nuclear factor- κ B,^{55,56} it is likely that TTP can indirectly regulate the expression of additional inflammatory genes within the stomach.

Surprisingly, despite the almost complete suppression of inflammatory infiltrates into the stomachs of ADX TTP Δ ARE mice, we found striking up-regulation of numerous inflammatory transcripts and pathways. Increased TTP specifically suppressed the innate immune response, while pathways associated with the adaptive immune response were not affected significantly. It has been postulated previously that TTP preferentially regulates the innate immune response. However, although myeloid-specific TTP KO mice have an abnormal inflammatory response when challenged with lipopolysaccharide, they do not phenocopy the spontaneous inflammatory pathologies that develop in the whole-body TTP KO.⁵⁷ Several studies have found that lymphocytes are dispensable for inducing SPEM development.^{11,17,39} Thus, even if TTP primarily suppresses the innate immune system, ADX-induced lymphocyte activation may be inconsequential for SPEM development.

Aberrant TNF production is associated with numerous inflammatory pathologies of the gastrointestinal tract.⁵⁸ *H pylori* infection potently induces TNF production, and *Tnf* KO mice are protected from SPEM development in some mouse models.^{11,41} Thus, TNF may contribute to gastric carcinogenesis. *Tnf* mRNA is a well-known TTP target, and

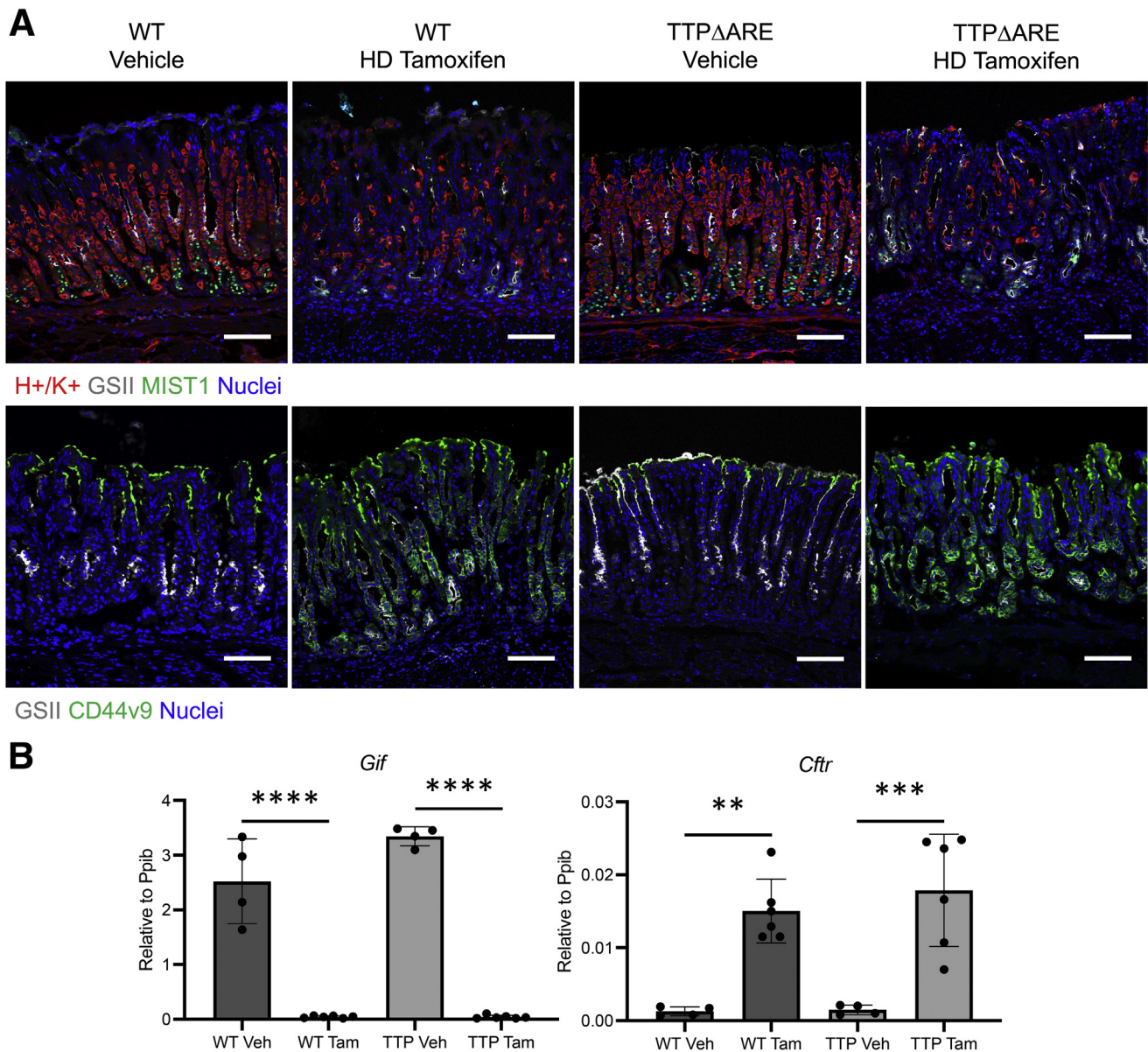


Figure 7. TTP overexpression does not affect high-dose-tamoxifen-induced SPEM development. (A) Representative immunostaining of the gastric corpus from WT and TTP Δ ARE homozygous mice treated with tamoxifen for 3 consecutive days. Gastric sections were probed for ATP4B (parietal cells, red), MIST1 (chief cells, green), and GSII lectin (mucous neck cells, grey); or with CD44v9 (SPEM, green) and GSII. Nuclei were stained with 4',6-diamidino-2-phenylindole. Scale bars: 100 μ m. $n \geq 5$ mice/group. (B) Quantitation of the number of parietal cells and chief cells observed per 20 \times field ($n \geq 6$ mice/group). Data are means \pm SD. P values were determined by 1-way analysis of variance with a post hoc Tukey t test. ** $P \leq .01$, *** $P \leq .001$, and **** $P \leq .0001$. Tam, tamoxifen; Veh, vehicle.

the numerous inflammatory pathologies that develop in TTP KO mice were rescued by treatment with TNF neutralizing antibodies^{25,52} or by breeding to TNF-receptor-deficient mice.⁵¹ Although macrophages produce large amounts of TNF and are critical for driving SPEM development,⁵⁷ we hypothesized that TTP suppression of *Tnf* was the underlying mechanism by which TTP Δ ARE mice were protected from ADX-induced gastric inflammation. Surprisingly, we found that *Tnf* KO mice were at least partially susceptible to ADX-induced gastric inflammation and metaplasia. Interestingly, *Tnf* KO mice did not develop ADX-induced

splenomegaly. These results show tissue-specific roles for TTP in regulating inflammation, and suggest that TTP's anti-inflammatory role in the stomach is more complex than the suppression of a single proinflammatory cytokine.

Regulation of inflammation is multifaceted, occurring at the transcriptional level, post-transcriptional level, and beyond. We previously have shown that glucocorticoids are critical transcriptional regulators of gastric inflammation.¹⁷ Here, we report that increased expression of the RNA binding protein TTP protects mice from gastric inflammation and metaplasia. Importantly, TTP transcription is

induced by glucocorticoids.⁵⁹ TTP may be a key effector molecule by which glucocorticoids regulate the gastric inflammatory response and may be a useful therapeutic target for treating gastric inflammatory disease. Recent reports have found that TTP expression is decreased in gastric cancer samples.²⁴ Thus, there is a need for continued study into the role of TTP in suppressing gastric inflammation and carcinogenesis.

Materials and Methods

Animal Care and Treatment

All mouse studies were performed with approval by the National Institute of Environmental Health Sciences Animal Care and Use Committee. C57BL/6J mice were purchased from the Jackson Laboratories (000664; Bar Harbor, MA). TTP Δ ARE mice were generated as previously described and were maintained on a congenic C57Bl/6 genetic background.²⁸ Mice were administered standard chow and water ad libitum and maintained in a temperature and humidity-controlled room with standard 12-hour light/dark cycles. Sham, adrenalectomy, and castration surgeries were performed at 8 weeks of age by the National Institute of Environmental Health Sciences Comparative Medicine Branch. After ADX, mice were maintained on 0.85% saline drinking water to maintain ionic homeostasis. HDT treatment was performed as previously described by Saenz et al.⁴⁴ Briefly, mice received 3 consecutive intraperitoneal injections of 0.25 mg/g body weight tamoxifen (MilliporeSigma, Burlington, MA) every 24 hours. Stomach tissue was collected 24 hours after the final dose.

Histology

Mice were euthanized by cervical dislocation at the indicated time points. Stomachs were removed and opened along the greater curvature and washed in phosphate-buffered saline to remove gastric contents. Stomachs were fixed overnight in 4% paraformaldehyde at 4°C and then cryopreserved in 30% sucrose and embedded in optimal cutting temperature media. Histology and cell quantitation were performed as previously described.¹⁷ Briefly, 5- μ m stomach cryosections were incubated with antibodies against the H+/K+ adenosine triphosphatase α subunit (clone 1H9; MBL International Corporation, Woburn, MA), MIST1 (clone D7N4B; Cell Signaling Technologies, Danvers, MA), CD45 (clone 104; BioLegend, San Diego, CA), CD44v9 (Cosmo Bio, Tokyo, Japan), CD68 (clone E307V; Cell Signaling Technologies), Siglec F (clone 1RNM44NN; eBiosciences, San Diego, CA), Ki67 (clone D3B5; Cell Signaling Technologies), or CTNNB1 (clone 14; BD BioSciences, Franklin Lakes, NJ) for 1 hour at room temperature or overnight at 4°C. After washing in phosphate-buffered saline with 0.1% Triton X-100 (Thermo Fisher Scientific, Waltham, MA), sections were incubated in secondary antibodies for 1 hour at room temperature. Fluorescent-conjugated GSII lectin (Thermo Fisher Scientific, Waltham, MA) was added with secondary antibodies. Sections were mounted with Vectastain mounting media containing 4',6-diamidino-2-phenylindole to visualize nuclei (Vector Laboratories,

Burlingame, CA). Images were obtained using a Zeiss 710 confocal laser-scanning microscope equipped with Airyscan (Carl-Zeiss GmbH, Jena, Germany) and running Zen Black (Carl-Zeiss GmbH) imaging software.

Image Quantitation

Parietal cells and chief cells were quantitated as previously described¹⁷ using confocal micrographs captured using a 20 \times microscope objective and 1- μ m-thick optical sections. Cells were counted using the ImageJ (National Institutes of Health, Bethesda, MD) count tool. Cells that stained positive with anti-H+/K+ antibodies were identified as parietal cells, while cells that stained positive with anti-MIST1 antibodies and were GSII negative were identified as mature chief cells. Counts were reported as the number of cells observed per 20 \times field. Images were chosen that contained gastric glands cut longitudinally. Leukocytes were quantitated using Nikon Elements General Analysis (Nikon, Tokyo, Japan). Six tile-scanned images were captured using the 20 \times objective and stitched on Zen Black. Eosinophils were identified as CD45/Siglec F double-positive, while macrophages were CD45/CD68 double-positive.

RNA Isolation and qRT-PCR

RNA used for qRT-PCR and RNAseq was isolated from a 4-mm biopsy specimen of the gastric corpus lesser curvature. RNA was extracted in TRIzol (Thermo Fisher Scientific) and precipitated from the aqueous phase using 1.5 volumes of 100% ethanol. The mixture was transferred to a RNeasy column (Qiagen, Hilden, Germany), and the remaining steps were followed according to the RNeasy kit manufacturer's recommendations. RNA was treated with RNase-free DNase I (Qiagen) as part of the isolation procedure. Reverse-transcription followed by qPCR was performed in the same reaction using the Universal Probes One-Step PCR kit (Bio-Rad Laboratories, Hercules, CA) and the TaqMan primers (Thermo Fisher Scientific) *Cftr* (Mm00445197_m1), *Olfm4* (Mm01320260_m1), *Wfdc2* (Mm00509434_m1), *Zfp36* (Mm00457144_m1), *Il33* (Mm00505403_m1), and *Il13* (Mm00434204_m1) (Thermo Fisher Scientific) on a Quantstudio 6 (Thermo Fisher Scientific). mRNA levels were normalized to the reference gene *Ppib* (Mm00478295_m1).

RNAseq

RNA was isolated 5 days after sham surgery or adrenalectomy as described earlier. Four mice were used for each experimental group. Indexed samples were sequenced using the 75-bp paired-end protocol via the NextSeq500 (Illumina) per the manufacturer's protocol. Raw reads (27–41 million pairs of reads per sample) were filtered using a custom perl script and the cutadapt program (v2.8) to remove low-quality reads and adapter sequences. Pre-processed reads were aligned to the University of California, Santa Cruz mm10 reference genome using STAR (v2.7.0f) with default parameters.⁶⁰ The quantification results from *featureCounts* (available in Subread software, v1.6.4) then were analyzed with the Bioconductor package DESeq2, which fits a negative binomial distribution to estimate

technical and biological variability.⁶¹ Comparisons were made between sham WT vs ADX WT, sham TTP Δ ARE vs ADX TTP Δ ARE, and ADX WT vs TTP Δ ARE. An abundance cut-off value was used so that only transcripts were evaluated whose average expression in the WT samples was greater than 0.1 fragments per kilobase of transcript per million mapped reads (FPKM). A transcript was considered differentially expressed if the adjusted *P* value was less than .05 and its expression changed -1.5-fold or less or 1.5-fold or more. Lists of significant transcripts were analyzed further using IPA (version 01-18-05; Qiagen). Enrichment or overlap was determined by IPA using the Fisher exact test ($P < .05$). GSEA was performed using GSEA v4.0.3 software (Broad Institute, San Diego, CA) and Molecular Signatures Database v7.0.⁶² Transcripts were preranked based on their *P* value and their fold change of gene expression. This application scores a sorted list of transcripts with respect to their enrichment in selected functional categories (KEGG, Biocarta, Reactome and GO). The significance of the enrichment score was assessed using 1000 permutations. Benjamini and Hochberg's false-discovery rate was calculated for multiple testing adjustments. A *q* value of 0.05 or less was considered significant. The heatmap was generated with the mean expression values of the 94 selected genes. The expression values were log₂-transformed before subjecting to heatmap generation with scale by row in the heatmap function available in R package pheatmap. The RNAseq data are available in the Gene Expression Omnibus repository at the National Center for Biotechnology Information (accession number: GSE164349; available at <https://www.ncbi.nlm.nih.gov/geo>).

Statistical Analysis

All error bars are \pm SD of the mean. The sample size for each experiment is indicated in the figure legends. Experiments were repeated a minimum of 2 times. Statistical analyses were performed using 1-way analysis of variance with the post hoc Tukey *t* test when comparing 3 or more groups or by an unpaired *t* test when comparing 2 groups. Statistical analysis was performed by GraphPad Prism 8 software (GraphPad Software, San Diego, CA). Statistical significance was set at $P \leq .05$. Specific *P* values are listed in the figure legends.

References

1. Torre LA, Bray F, Siegel RL, Ferlay J, Lortet-Tieulent J, Jemal A. Global cancer statistics, 2012. *CA Cancer J Clin* 2015;65:87–108.
2. Peek RM Jr, Blaser MJ. *Helicobacter pylori* and gastrointestinal tract adenocarcinomas. *Nat Rev Cancer* 2002; 2:28–37.
3. Landgren AM, Landgren O, Gridley G, Dores GM, Linet MS, Morton LM. Autoimmune disease and subsequent risk of developing alimentary tract cancers among 4.5 million US male veterans. *Cancer* 2011;117:1163–1171.
4. Petersen CP, Mills JC, Goldenring JR. Murine models of gastric corpus preneoplasia. *Cell Mol Gastroenterol Hepatol* 2017;3:11–26.
5. Yoshizawa N, Takenaka Y, Yamaguchi H, Tetsuya T, Tanaka H, Tatematsu M, Nomura S, Goldenring JR, Kaminishi M. Emergence of spasmolytic polypeptide-expressing metaplasia in Mongolian gerbils infected with *Helicobacter pylori*. *Lab Invest* 2007;87:1265–1276.
6. Correa P, Shiao YH. Phenotypic and genotypic events in gastric carcinogenesis. *Cancer Res* 1994; 54(Suppl):1941s–1943s.
7. Meyer AR, Goldenring JR. Injury, repair, inflammation and metaplasia in the stomach. *J Physiol* 2018; 596:3861–3867.
8. Bockerstett KA, DiPaolo RJ. Regulation of gastric carcinogenesis by inflammatory cytokines. *Cell Mol Gastroenterol Hepatol* 2017;4:47–53.
9. Syu LJ, El-Zaatari M, Eaton KA, Liu Z, Tetarbe M, Keeley TM, Pero J, Ferris J, Wilbert D, Kaatz A, Zheng X, Qiao X, Grachtchouk M, Gumucio DL, Merchant JL, Samuelson LC, Dlugosz AA. Transgenic expression of interferon-gamma in mouse stomach leads to inflammation, metaplasia, and dysplasia. *Am J Pathol* 2012; 181:2114–2125.
10. Tu S, Bhagat G, Cui G, Takaishi S, Kurt-Jones EA, Rickman B, Betz KS, Penz-Oesterreicher M, Bjorkdahl O, Fox JG, Wang TC. Overexpression of interleukin-1beta induces gastric inflammation and cancer and mobilizes myeloid-derived suppressor cells in mice. *Cancer Cell* 2008;14:408–419.
11. Oshima M, Oshima H, Matsunaga A, Taketo MM. Hyperplastic gastric tumors with spasmolytic polypeptide-expressing metaplasia caused by tumor necrosis factor-alpha-dependent inflammation in cyclooxygenase-2/microsomal prostaglandin E synthase-1 transgenic mice. *Cancer Res* 2005; 65:9147–9151.
12. Osaki LH, Bockerstett KA, Wong CF, Ford EL, Madison BB, DiPaolo RJ, Mills JC. Interferon- γ directly induces gastric epithelial cell death and is required for progression to metaplasia. *J Pathol* 2019;247:513–523.
13. Bockerstett KA, Petersen CP, Noto CN, Kuehm LM, Wong CF, Ford EL, Teague RM, Mills JC, Goldenring JR, DiPaolo RJ. Interleukin 27 protects from gastric atrophy and metaplasia during chronic autoimmune gastritis. *Cell Mol Gastroenterol Hepatol* 2020;10:561–579.
14. El-Omar EM, Rabkin CS, Gammon MD, Vaughan TL, Risch HA, Schoenberg JB, Stanford JL, Mayne ST, Goedert J, Blot WJ, Fraumeni JF Jr, Chow WH. Increased risk of noncardia gastric cancer associated with proinflammatory cytokine gene polymorphisms. *Gastroenterology* 2003;124:1193–1201.
15. Lee CW, Rao VP, Rogers AB, Ge Z, Erdman SE, Whary MT, Fox JG. Wild-type and interleukin-10-deficient regulatory T cells reduce effector T-cell-mediated gastroduodenitis in Rag2^{-/-} mice, but only wild-type regulatory T cells suppress *Helicobacter pylori* gastritis. *Infect Immun* 2007;75:2699–2707.
16. Busada JT, Peterson KN, Khadka S, Xu X, Oakley RH, Cook DN, Cidlowski JA. Glucocorticoids and androgens protect from gastric metaplasia by suppressing group 2 innate lymphoid cell activation. *Gastroenterology* 2021; 161:637–652.e4.

17. Busada JT, Ramamoorthy S, Cain DW, Xu X, Cook DN, Cidlowski JA. Endogenous glucocorticoids prevent gastric metaplasia by suppressing spontaneous inflammation. *J Clin Invest* 2019;129:1345–1358.
18. DuBois RN, McLane MW, Ryder K, Lau LF, Nathans D. A growth factor-inducible nuclear protein with a novel cysteine/histidine repetitive sequence. *J Biol Chem* 1990;265:19185–19191.
19. Blackshear PJ. Tristetraprolin and other CCCH tandem zinc-finger proteins in the regulation of mRNA turnover. *Biochem Soc Trans* 2002;30:945–952.
20. Lai WS, Carballo E, Strum JR, Kennington EA, Phillips RS, Blackshear PJ. Evidence that tristetraprolin binds to AU-rich elements and promotes the deadenylation and destabilization of tumor necrosis factor alpha mRNA. *Mol Cell Biol* 1999;19:4311–4323.
21. Brooks SA, Blackshear PJ. Tristetraprolin (TTP): interactions with mRNA and proteins, and current thoughts on mechanisms of action. *Biochim Biophys Acta* 2013;1829:666–679.
22. Fu M, Blackshear PJ. RNA-binding proteins in immune regulation: a focus on CCCH zinc finger proteins. *Nat Rev Immunol* 2017;17:130–143.
23. Saini Y, Chen J, Patial S. The tristetraprolin family of RNA-binding proteins in cancer: progress and future prospects. *Cancers (Basel)* 2020;12:1539.
24. Deng K, Wang H, Shan T, Chen Y, Zhou H, Zhao Q, Xia J. Tristetraprolin inhibits gastric cancer progression through suppression of IL-33. *Sci Rep* 2016;6:24505.
25. Taylor GA, Carballo E, Lee DM, Lai WS, Thompson MJ, Patel DD, Schenkman DI, Gilkeson GS, Broxmeyer HE, Haynes BF, Blackshear PJ. A pathogenetic role for TNF alpha in the syndrome of cachexia, arthritis, and autoimmunity resulting from tristetraprolin (TTP) deficiency. *Immunity* 1996;4:445–454.
26. Cao H, Tuttle JS, Blackshear PJ. Immunological characterization of tristetraprolin as a low abundance, inducible, stable cytosolic protein. *J Biol Chem* 2004;279:21489–21499.
27. Tchen CR, Brook M, Saklatvala J, Clark AR. The stability of tristetraprolin mRNA is regulated by mitogen-activated protein kinase p38 and by tristetraprolin itself. *J Biol Chem* 2004;279:32393–32400.
28. Patial S, Curtis AD 2nd, Lai WS, Stumpo DJ, Hill GD, Flake GP, Mannie MD, Blackshear PJ. Enhanced stability of tristetraprolin mRNA protects mice against immune-mediated inflammatory pathologies. *Proc Natl Acad Sci U S A* 2016;113:1865–1870.
29. Choudhary I, Vo T, Bathula CS, Lamichhane R, Lewis BW, Looper J, Jeyaseelan S, Blackshear PJ, Saini Y, Patial S. Tristetraprolin overexpression in non-hematopoietic cells protects against acute lung injury in mice. *Front Immunol* 2020;11:2164.
30. Steinkamp HM, Hathaway-Schrader JD, Chavez MB, Aartun JD, Zhang L, Jensen T, Shojaee Bakhtiari A, Helke KL, Stumpo DJ, Alekseyenko AV, Novince CM, Blackshear PJ, Kirkwood KL. Tristetraprolin is required for alveolar bone homeostasis. *J Dent Res* 2018;97:946–953.
31. Xu B, Tang J, Lyu C, Wandu W, Stumpo D, Mattapallil M, Caspi R, Blackshear P, Gery I. Regulated tristetraprolin (TTP) overexpression dampens the development and pathogenesis of experimental autoimmune uveitis (EAU). *Front Immunol* 2021;11:583510.
32. Assabban A, Dubois-Vedrenne I, Van Maele L, Salcedo R, Snyder B, Zhou LAA, de Toef BLG, La CMM, Nguyen MTS, Fan WS, Hu W, Blanpain C, Trinchieri G, Gueydan C, Blackshear PJ, Goriely S. Tristetraprolin expression by keratinocytes protects against skin carcinogenesis. *JCI Insight* 2021;6:e140669.
33. Saenz JB, Mills JC. Acid and the basis for cellular plasticity and reprogramming in gastric repair and cancer. *Nat Rev Gastroenterol Hepatol* 2018;15:257–273.
34. Bertaux-Skeirik N, Wunderlich M, Teal E, Chakrabarti J, Biesiada J, Mahe M, Sundaram N, Gabre J, Hawkins J, Jian G, Engevik AC, Yang L, Wang J, Goldenring JR, Qualls JE, Medvedovic M, Helmrath MA, Diwan T, Mulloy JC, Zavros Y. CD44 variant isoform 9 emerges in response to injury and contributes to the regeneration of the gastric epithelium. *J Pathol* 2017;242:463–475.
35. Miao ZF, Sun JX, Adkins-Threats M, Pang MJ, Zhao JH, Wang X, Tang KW, Wang ZN, Mills JC. DDIT4 licenses only healthy cells to proliferate during injury-induced metaplasia. *Gastroenterology* 2021;160:260–271.e10.
36. Willet SG, Lewis MA, Miao ZF, Liu D, Radyk MD, Cunningham RL, Burclaff J, Sibbel G, Lo HG, Blanc V, Davidson NO, Wang ZN, Mills JC. Regenerative proliferation of differentiated cells by mTORC1-dependent paligenesis. *EMBO J* 2018;37:e98311.
37. Lee HJ, Nam KT, Park HS, Kim MA, Lafleur BJ, Aburatani H, Yang HK, Kim WH, Goldenring JR. Gene expression profiling of metaplastic lineages identifies CDH17 as a prognostic marker in early stage gastric cancer. *Gastroenterology* 2010;139:213–225.e3.
38. Weis VG, Sousa JF, LaFleur BJ, Nam KT, Weis JA, Finke PE, Ameen NA, Fox JG, Goldenring JR. Heterogeneity in mouse spasmolytic polypeptide-expressing metaplasia lineages identifies markers of metaplastic progression. *Gut* 2013;62:1270–1279.
39. Petersen CP, Weis VG, Nam KT, Sousa JF, Fingleton B, Goldenring JR. Macrophages promote progression of spasmolytic polypeptide-expressing metaplasia after acute loss of parietal cells. *Gastroenterology* 2014;146:1727–1738.e8.
40. Petersen CP, Meyer AR, De Salvo C, Choi E, Schlegel C, Petersen A, Engevik AC, Prasad N, Levy SE, Peebles RS, Pizarro TT, Goldenring JR. A signalling cascade of IL-33 to IL-13 regulates metaplasia in the mouse stomach. *Gut* 2018;67:805–817.
41. Crabtree JE, Shallcross TM, Heatley RV, Wyatt JI. Mucosal tumour necrosis factor alpha and interleukin-6 in patients with Helicobacter pylori associated gastritis. *Gut* 1991;32:1473–1477.
42. Streng CB, Nathan P. The immune response in steroid deficient mice. *Immunology* 1973;24:559–565.
43. Huh WJ, Khurana SS, Geahlen JH, Kohli K, Waller RA, Mills JC. Tamoxifen induces rapid, reversible atrophy,

- and metaplasia in mouse stomach. *Gastroenterology* 2012;142:21–24.e7.
44. Saenz JB, Burclaff J, Mills JC. Modeling murine gastric metaplasia through tamoxifen-induced acute parietal cell loss. *Methods Mol Biol* 2016;1422:329–339.
 45. Brinegar AE, Cooper TA. Roles for RNA-binding proteins in development and disease. *Brain Res* 2016;1647:1–8.
 46. Brewer BY, Malicka J, Blackshear PJ, Wilson GM. RNA sequence elements required for high affinity binding by the zinc finger domain of tristetraprolin: conformational changes coupled to the bipartite nature of Au-rich mRNA-destabilizing motifs. *J Biol Chem* 2004;279:27870–27877.
 47. Wells ML, Huang W, Li L, Gerrish KE, Fargo DC, Oszolak F, Blackshear PJ. Posttranscriptional regulation of cell-cell interaction protein-encoding transcripts by Zfs1p in *Schizosaccharomyces pombe*. *Mol Cell Biol* 2012;32:4206–4214.
 48. Newman R, McHugh J, Turner M. RNA binding proteins as regulators of immune cell biology. *Clin Exp Immunol* 2016;183:37–49.
 49. Brennan SE, Kuwano Y, Alkharouf N, Blackshear PJ, Gorospe M, Wilson GM. The mRNA-destabilizing protein tristetraprolin is suppressed in many cancers, altering tumorigenic phenotypes and patient prognosis. *Cancer Res* 2009;69:5168–5176.
 50. Bakheet T, Williams BR, Khabar KS. ARED 3.0: the large and diverse AU-rich transcriptome. *Nucleic Acids Res* 2006;34:D111–D114.
 51. Carballo E, Blackshear PJ. Roles of tumor necrosis factor- α receptor subtypes in the pathogenesis of the tristetraprolin-deficiency syndrome. *Blood* 2001;98:2389–2395.
 52. Carballo E, Lai WS, Blackshear PJ. Feedback inhibition of macrophage tumor necrosis factor- α production by tristetraprolin. *Science* 1998;281:1001–1005.
 53. Meyer AR, Engevik AC, Madorsky T, Belmont E, Stier MT, Norlander AE, Pilkinton MA, McDonnell WJ, Weis JA, Jang B, Mallal SA, Peebles RS Jr, Goldenring JR. Group 2 innate lymphoid cells coordinate damage response in the stomach. *Gastroenterology* 2020;159:2077–2091.e8.
 54. Jeong H, Lee B, Kim KH, et al. WFDC2 promotes spasmolytic polypeptide-expressing metaplasia through the upregulation of IL33 in response to injury. *Gastroenterology* 2021;161(3):953–967.
 55. Liang J, Lei T, Song Y, Yanes N, Qi Y, Fu M. RNA-destabilizing factor tristetraprolin negatively regulates NF- κ B signaling. *J Biol Chem* 2009;284:29383–29390.
 56. Schichl YM, Resch U, Hofer-Warbinek R, de Martin R. Tristetraprolin impairs NF- κ B/p65 nuclear translocation. *J Biol Chem* 2009;284:29571–29581.
 57. Qiu LQ, Stumpo DJ, Blackshear PJ. Myeloid-specific tristetraprolin deficiency in mice results in extreme lipopolysaccharide sensitivity in an otherwise minimal phenotype. *J Immunol* 2012;188:5150–5159.
 58. Delgado ME, Brunner T. The many faces of tumor necrosis factor signaling in the intestinal epithelium. *Genes Immun* 2019;20:609–626.
 59. Smoak K, Cidlowski JA. Glucocorticoids regulate tristetraprolin synthesis and posttranscriptionally regulate tumor necrosis factor α inflammatory signaling. *Mol Cell Biol* 2006;26:9126–9135.
 60. Dobin A, Davis CA, Schlesinger F, Drenkow J, Zaleski C, Jha S, Batut P, Chaisson M, Gingeras TR. STAR: ultrafast universal RNA-seq aligner. *Bioinformatics* 2013;29:15–21.
 61. Love MI, Huber W, Anders S. Moderated estimation of fold change and dispersion for RNA-seq data with DESeq2. *Genome Biol* 2014;15:550.
 62. Subramanian A, Tamayo P, Mootha VK, Mukherjee S, Ebert BL, Gillette MA, Paulovich A, Pomeroy SL, Golub TR, Lander ES, Mesirov JP. Gene set enrichment analysis: a knowledge-based approach for interpreting genome-wide expression profiles. *Proc Natl Acad Sci U S A* 2005;102:15545–15550.

Received January 25, 2021. Accepted July 27, 2021.

Correspondence

Address correspondence to: Jonathan T. Busada, PhD, Department of Microbiology, Immunology and Cell Biology, West Virginia University School of Medicine, 64 Medical Center Drive, PO Box 9177, Morgantown, West Virginia 26506. e-mail: jonathan.busada@hsc.wvu.edu.

Acknowledgments

The authors thank the National Institute of Environmental Health Sciences Comparative Medicine Branch, Epigenomes Core Laboratory, and Fluorescence Microscopy and Imaging Center for their assistance. The authors also thank Michael Fessler and Donald Cook for critical reading of the manuscript.

CRedit Authorship Contributions

Jonathan T Busada, PhD (Conceptualization: Lead; Data curation: Lead; Formal analysis: Lead; Funding acquisition: Equal; Project administration: Lead; Writing – original draft: Lead)
 Stuti Khadka (Data curation: Equal; Formal analysis: Equal; Writing – review & editing: Supporting)
 Kylie N Peterson (Data curation: Supporting; Formal analysis: Supporting; Writing – review & editing: Supporting)
 Sara R Druffner (Data curation: Supporting; Formal analysis: Supporting; Investigation: Supporting)
 Deborah J Stumpo (Data curation: Supporting; Methodology: Equal)
 Lecong Zhou (Data curation: Equal; Formal analysis: Equal; Visualization: Equal; Writing – review & editing: Supporting)
 Robert H Oakley (Data curation: Supporting; Formal analysis: Supporting; Investigation: Supporting)
 John A Cidlowski (Funding acquisition: Equal; Methodology: Equal; Resources: Equal; Writing – review & editing: Supporting)
 Perry J Blackshear (Conceptualization: Equal; Formal analysis: Equal; Funding acquisition: Equal; Writing – original draft: Equal)

Conflicts of interest

The authors disclose no conflicts.

Funding

This research was supported by the National Institute of General Medical Sciences 1F12GM123974 (J.T.B.) and P20GM121322 (J.T.B.), West Virginia University start-up funds (J.T.B.), and by the Intramural Research Program of the National Institutes of Health/National Institute of Environmental Health Sciences 1ZIAES090057 (J.A.C) and 1ZIAES090080 (P.J.B.). Confocal microscopy was performed at the West Virginia University Microscope Imaging Facility, which is supported by National Institutes of Health grants P20RR016440, P30GM103488, U54GM104942, P30GM103503, and P20GM103434.